Morphosynthesis of Nanostructured Polymer Gels by Polymerization within Reverse Hexagonal Mesophases

Hans-Peter Hentze and Eric W. Kaler*

Center for Molecular Engineering and Thermodynamics, Department of Chemical Engineering, University of Delaware, Newark, Delaware 19711

Received August 19, 2002. Revised Manuscript Received December 4, 2002

Free radical polymerization of divinyl benzene (DVB) and styrene (St) was performed within reverse hexagonal phases of the anionic surfactant bis(2-ethylhexyl) sulfosuccinate sodium salt (AOT). The morphologies before and after polymerization were studied by small-angle X-ray scattering (SAXS), polarized light microscopy, and scanning and transmission electron microscopy. Polarized light microscopy and SAXS show no significant changes in textures and order during polymerization. A detailed investigation of the polymer matrix after polymerization and removal of the template reveals the formation of regular micrometer-sized layerlike morphologies. The polymer layers have a hierarchical structure, as they consist of aligned strings of polymer beads with diameters of about 100 nm. Structure formation is directed by the lyotropic phase during polymerization-induced phase separation on a nanometer scale. A mechanism of morphosynthesis is discussed on the basis of characteristic distortions within liquid crystals that are induced by the polymer phase. Parameters such as cross-linking degree and initiator or monomer concentration have a strong influence on the morphologies formed due to a kinetically controlled nucleation and growth mechanism. Finally, the structures formed by polymerization within reverse hexagonal phases are compared to those obtained from lamellar phases of the same surfactant.

I. Introduction

Nanostructured organic polymer gels are promising materials for a wide range of applications, such as supports for catalysts, sorbents, reactive membranes, chromatography, or drug delivery, or as components of nanocomposite materials. Compared to their inorganic counterparts they typically exhibit different mechanical and chemical properties such as elasticity or mechanical and chemical resistance, and they can be easily functionalized by copolymerization or polymer-analogous reactions. A convenient way to obtain nanostructured polymers is by the use of templates. In a wide sense templates are structure-directing agents. The different templating approaches described in the literature show the versatility of templating techniques. Generally, three different cases can be distinguished[1] (Figure 1).

In synergistic synthesis the monomer is the only, or at least one of, the self-assembling entities forming the long-range ordered template. After polymerization the parental order is retained, and the product can be best described as a polymerized self-assembled template structure. This is the most common approach for templating organic polymers in lyotropic phases,[2−11] even though not all attempts successfully retain the template structure. In addition to the use of polymerizable surfactants for this templating, the slow exchange dynamics and high cross-linking degrees available in lyotropic mesophases of amphiphilic block copolymers containing reactive entities make them especially suitable for preserving the initial template structure.[12−16]

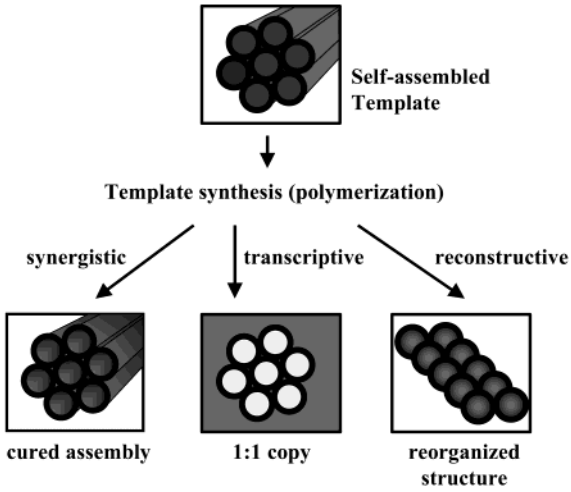

Figure 1. Scheme of various templating approaches.

* To whom correspondence should be addressed. Phone: 302-831-3553. Fax: 302-831-6751. E-mail: kaler@che.udel.edu.

(1) Mann, S.; Burkett, S. L.; Davis, S. A.; Fowler, C. E.; Mendelson, N. H.; Sims, S. D.; Walsh, D.; Whilton, N. T. *Chem. Mater.* **1997**, *9*, 2300.
(2) Friberg, S. E.; Thundathil, R.; Stoffer, J. O. *Science* **1979**, *205*, 607.
(3) McGrath, K. M. *Colloid Polym. Sci.* **1996**, *274*, 499.
(4) McGrath, K. M. *Colloid Polym. Sci.* **1996**, *274*, 399.
(5) McGrath, K. M.; Drummond, C. J. *Colloid Polym. Sci.* **1996**, *274*, 612.
(6) McGrath, K. M.; Drummond, C. J. *Colloid Polym. Sci.* **1996**, *274*, 316.
(7) Pindzola, B. A.; Hoag, B. P.; Gin, D. L. *J. Am. Chem. Soc.* **2001**, *123*, 4617.
(8) Deng, H.; Gin, D. L.; Smith, R. C. *J. Am. Chem. Soc.* **1998**, *120*, 3522.

10.1021/cm020832r CCC: $25.00
Published on Web 01/16/2003

Transcriptive synthesis is a second approach to templating, and here also the parental structure is retained during polymerization. Unlike synergistic approaches, the monomer is not part of the self-assembled aggregates and the final material is a direct cast of the template. In some cases the organic polymer structure is retained by transcriptive synthesis.[17,18] These materials were investigated before and after polymerization, but the template was not removed after polymerization.

If the final product is ordered but does not retain the parental structure an indirect templating or reconstructive morphosynthesis has occurred. Here the template acts only as a structure *directing* agent. In these cases changes in morphology compared to the template structure occur mainly for thermodynamic reasons. Generally, the phase behavior of the polymerized system (e.g., polymer/surfactant/water) is dramatically different from that of the nonpolymerized system (e.g., monomer/surfactant/water). Therefore, monomer consumption on one hand and polymer formation on the other usually have a strong influence on the self-assembled morphologies. Furthermore, for entropic reasons the polymer chains formed tend to coil and so do not easily adapt to the confined geometry of the template. Indirect templating often leads to complex polymer morphologies, usually structured somewhere in the nanometer to micrometer range. An example of reconstructive morphosynthesis of organic polymers by lyotropic templating is the cross-linking polymerization of acrylamide within hexagonal phases of cetyltrimethylammonium surfactants.[19] The result is sheetlike polymer morphologies.

Here, the reconstructive morphosynthesis of polymer gels within aqueous solutions of bis(2-ethylhexyl) sulfosuccinate sodium salt (AOT) is described. Polymerization of styrene and divinyl benzene (DVB) was carried out within the hydrophobic domains of reverse hexagonal and lamellar lyotropic phases of the template. The samples were characterized before and after polymerization by imaging and scattering techniques, i.e., polarized light microscopy (POM) and small-angle X-ray scattering (SAXS). Scanning (SEM) and transmission electron microscopy (TEM) as well as SAXS were used for a detailed investigation of the polymer morphologies after removal of the template. A mechanistic model is proposed to explain the observed structure formation by characteristic distortions within liquid-crystalline phases induced by the formation of a phase-separating polymer phase.

II. Experimental Section

II.1. Materials. Bis(2-ethylhexyl) sulfosuccinate sodium salt (AOT), potassium peroxodisulfate (KPS), 2,2′-azobis(2-methylpropionitrile) (AIBN), and ethanol were all purchased from Aldrich Co. and used as received. Divinyl benzene and styrene (both from Aldrich) were distilled under reduced pressure to remove inhibitors. Deionized water (Milli-Q) was used for the preparation of lyotropic AOT phases.

II.2. Polymerization of Lyotropic Mesophases and Purification of Polymer Gels. Lyotropic solutions were prepared by mechanical mixing of AOT and water, followed by centrifugation to remove air bubbles using a Hettrich Universal centrifuge at a speed of 2000 rpm. KPS was added as an 18 wt % aqueous solution. In the case of AIBN the initiator was dissolved in the monomer mixture. The homogenization procedure by mechanical homogenization and centrifugation was repeated three times before and after addition of monomer and initiator. The lyotropic mixtures containing all reactants were equilibrated overnight at room temperature, subsequently characterized by POM and SAXS, and polymerized at 60 °C for 24 h. After polymerization, the template was removed by ultrafiltration using Schleicher & Schuell 300-mL ultrafiltration cells, Ultran RC/100 (Schleicher & Schuell) membranes, and ethanol as the eluent.

II.3. Analytical Methods. *Optical Microscopy*. Polarized light optical microscopy (POM) was used to characterize the lyotropic phases before and after polymerization. An Olympus BX50 optical microscope was connected to a Linkam THL 60/8/6R hotstage for temperature control. Thin films of the lyotropic phases were heated between glass slides from 25 up to 60 °C.

Small-Angle X-ray Scattering. Small-angle X-ray scattering (SAXS) was performed using a Kratky camera (Fa. Paar). Samples of the lyotropic phases were placed between polymer foil and measured under Helium atmosphere to avoid water evaporation. The polymerized samples and the purified polymer gels were measured under the same conditions. The scattering vector q is defined as $q = 2\pi(2/\lambda)\sin(\theta/2)$, where θ is the scattering angle. The measurements were performed in a q range of 1×10^{-2} nm$^{-1} < q/2\,\pi < 9.0 \times 10^{-1}$ nm^{-1}.

Electron Microscopy. After removing the template by ultrafiltration, the purified polymer gels were investigated by transmission electron microscopy (TEM) using a Zeiss EM 912 OMEGA microscope, operating at an acceleration voltage of 120 kV. For scanning electron microscopy (SEM) the purified samples were placed on carbon coated stubs, sputter coated, and characterized using a Zeiss DSM 940 microscope.

III. Results and Discussion

Polymerization within Reverse Hexagonal Phases. Lyotropic phases were prepared by mixing and mechanical homogenization of the reactants at room temperature. Subsequently all samples were characterized by polarized light microscopy at 25 and 60 °C. The samples used for polymerization all showed the same phase morphology (inverse hexagonal or lamellar) within this temperature range (Table 1). Swelling of the binary phases with different amounts of monomer did not result in phase transitions in the concentration range investigated as shown by POM and SAXS.

Before polymerization all samples appeared translucent. Within the inverse hexagonal phase region the viscosity is very high, and fan textures typical for hexagonal phases were observed by POM (Figure 2a). The SAXS diffractogram of the template (AOT/water) shows the characteristic pattern for hexagonal phases with peak distances of $1{:}\sqrt{3}{:}\sqrt{4}$ (Figure 3). The first-order peak can be correlated to a d-spacing of 2.29 nm. After swelling with monomer the first-order peak is

(9) Resel, R.; Leising, G.; Markart, P.; Kriechbaum, M.; Smith, R.; Gin, D. *Macromol. Chem. Phys.* **2000**, *201*, 1128.
(10) Reppy, M. A.; Gray, D. H.; Pindzola, B. A.; Smithers, J. L.; Gin, D. L. *J. Am. Chem. Soc.* **2001**, *123*, 363.
(11) Lee, Y. S.; Yang, J. Z.; Sisson, T. M.; Frankel, D. A.; Gleeson, J. T.; Aksay, E.; Keller, S. L.; Gruner, S. M.; O'Brien, D. F. *J. Am. Chem. Soc.* **1995**, *117*, 5573.
(12) Hentze, H.-P.; Krämer, E.; Berton, B.; Förster, S.; Antonietti, M.; Dreja, M. *Macromolecules* **1999**, *32*, 5803.
(13) Förster, S.; Berton, B.; Hentze, H.-P.; Krämer, E.; Antonietti, M.; Lindner, P. *Macromolecules* **2001**, *34*, 4610.
(14) Suvegh, K.; Domjan, A.; Vanko, G.; Ivan, B.; Vertes, A. *Macromolecules* **1998**, *31*, 7770.
(15) Ivan, B.; Almdal, K.; Mortensen, K.; Johannsen, I.; Kops, J. *Macromolecules* **2001**, *34*, 1579.
(16) Vamvakaki, M.; Patrickios, C. S. *Chem. Mater.* **2002**, *14*, 1630.
(17) Strom, P.; Anderson, D. M. *Langmuir* **1992**, *8*, 691.
(18) Laversanne, R. *Macromolecules* **1992**, *25*, 489.
(19) Antonietti, M.; Göltner, C.; Hentze, H.-P. *Langmuir* **1998**, *14*, 2670.

Table 1. Compositions of Samples Explored

sample	*m* AOT	*m* H_2O	*m* DVB	*m* styrene	*m* initiator	remarks
UDH 12	4.5 g	0.5 g	0.225 g		36 mg KPS	low c (DVB)
UDH 14	4.5 g	0.5 g	0.450 g		36 mg KPS	high c (DVB)
UDH 22	4.5 g	0.5 g	0.113 g	0.113 g	36 mg KPS	*m* DVB:*m* St = 1
UDH 24	4.5 g	0.5 g		0.225 g	36 mg KPS	no cross-linker
UDH 31	4.5 g	0.5 g	0.225 g		18 mg KPS	low c (Initiator)
UDH 34	4.5 g	0.5 g	0.225 g		180 mg KPS	high c (initiator)
UDH 35	4.5 g	0.5 g	0.225 g		36 mg AIBN	AIBN as initiator
UDH 62	3.6 g	1.2 g	0.225 g		36 mg KPS	lamellar phase

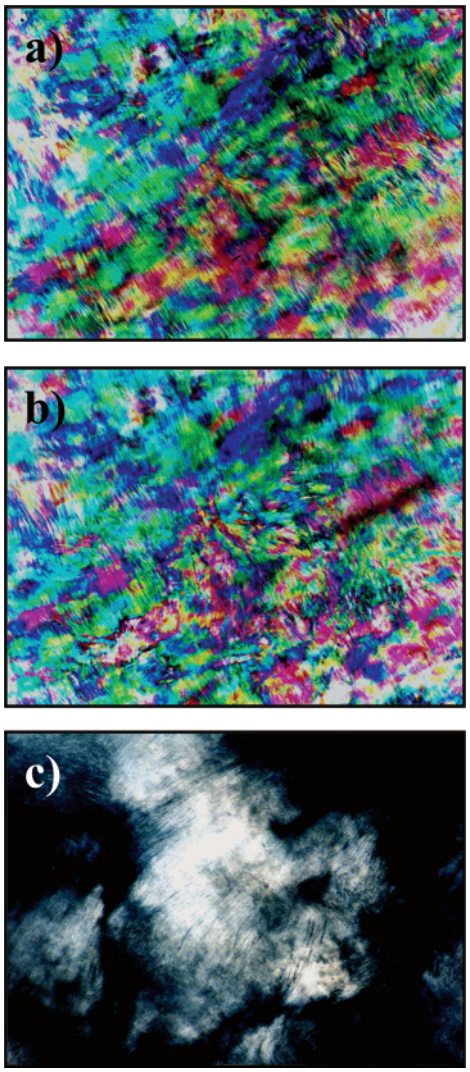

Figure 2. Polarized light micrographs of sample UDH 12: (a) before polymerization; (b) after polymerization; and (c) after removing the template by extraction with ethanol.

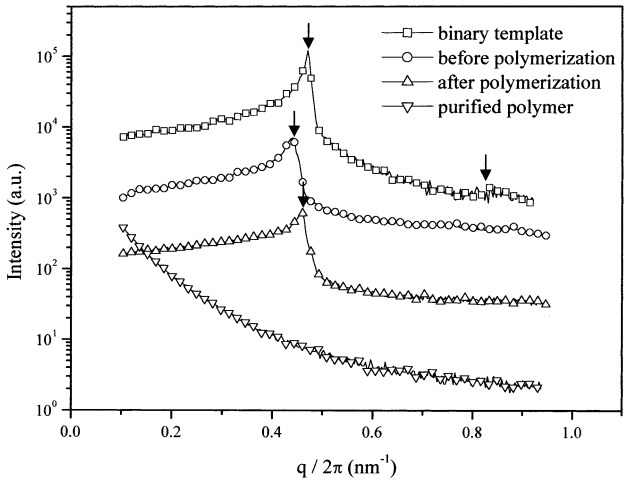

Figure 3. SAXS diffractograms of the binary template (AOT/water) (−□−), sample UDH 12 before (−○−) and after (−△−) polymerization, and of the purified, template-free polymer (−▽−). The arrows mark the first-order peak, and in case of the binary template arrows also mark the indexing of the second-order peak.

shifted to lower scattering vectors, indicating a small increase of the *d*-spacing to 2.39 nm for sample UDH12.

Free radical cross-linking polymerization was induced thermally at 60 °C. During polymerization no macroscopic phase-separation was observed, and there was only a slight increase in turbidity with increasing polymer content due to the increase in optical density during polymerization. No significant changes in morphologies were found before and after polymerization by POM (Figure 2b) and SAXS. A slight broadening of the SAXS peak indicated a small decrease in the degree of periodic order (Figure 3).

After polymerization the polymer matrix was purified by ultrafiltration and investigated. After removal of the template, SAXS showed that the purified polymer matrix had no periodic long-range order. Because a sharp scattering peak was observed after polymerization, it is likely that there is coexistence of a less-ordered polymer matrix with the highly ordered template phase after polymerization and before extraction. In polarized optical microscopy the purified polymer still appeared birefringent (Figure 2c). Although there is no characteristic texture (such as a fan texture), the birefringence suggests there is an anisotropic mesostructured polymer morphology. In contrast to the structure of dense, nontemplated polystyrene gels, SEM of the templated material reveals a layerlike polymer morphology (Figure 4). TEM indicates that these polymer sheets are built up hierarchically, as each single layer consists of strands of polymer beads with diameters of about 100 nm (Figure 5). The long-range order is relatively weak, so SAXS of the purified polymers showed no periodic scattering patterns.

Although macroscopic phase separation did not occur during polymerization, electron microscopy clearly shows demixing of the polymer phase from the lyotropic phase on a mesoscopic length scale. This idea is supported by the observed shift of the SAXS peak after polymerization toward the position measured for the binary AOT/water mixture. During polymerization the *d*-spacing decreased from 2.39 to 2.32 nm (Figure 3). The difference of about 70% compared to the binary system (AOT/water: 2.29 nm) is too large to be caused only by shrinkage due to the polymerization.

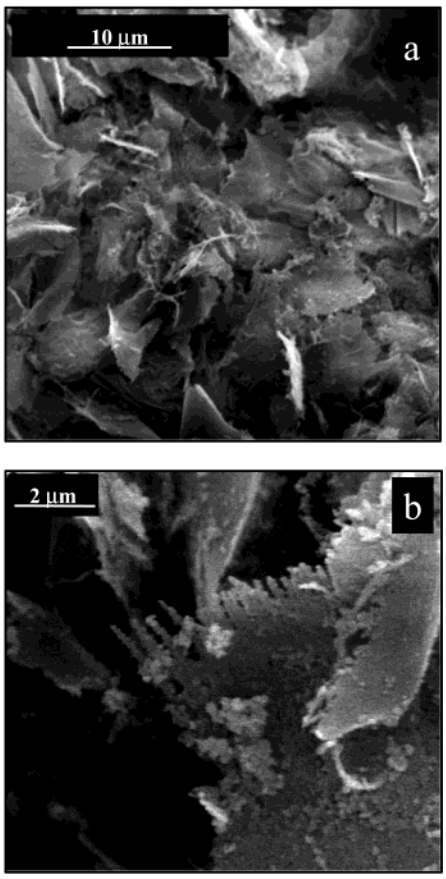

Figure 4. SEM micrographs of sample UDH 12 after removing the template. The purified polymer matrix consists of micrometer-sized sheetlike structures.

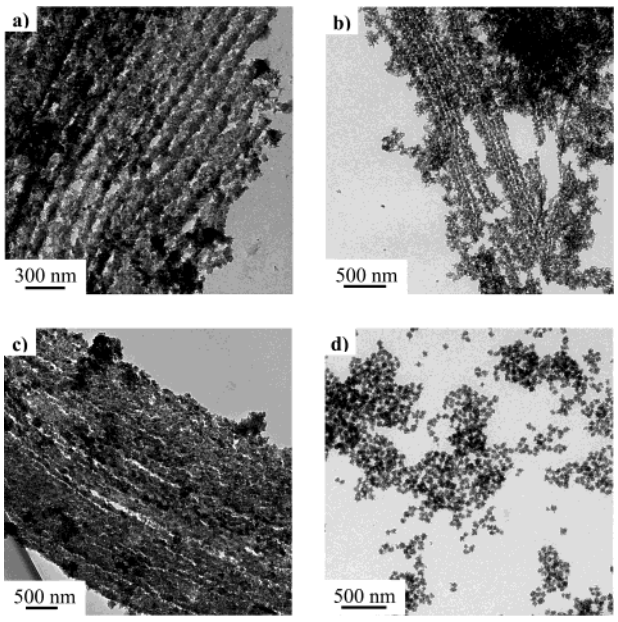

Figure 5. TEM micrographs: (a) the polymer sheets consist of chains of polymer clusters (UDH 12); (b) the chains have an extension of some micrometers (UDH 12); (c) at high monomer contents the structure becomes more dense (UDH 14); and (d) no long-range structure is observed for templating in the lamellar phase (UDH 62).

Proposed Mechanism of Morphosynthesis. The original nanostructure is not retained during the course of reaction, but instead hierarchical and regular polymer morphologies formed on a nano- to micrometer scale. Starting from a thermodynamically stable, self-organized lyotropic mesophase, polymer formation is directed by the reaction and results in an anisotropic polymer morphology. Because the polymer structure formation takes place on a length scale much larger than the characteristic length of the template, the confined geometry of the template aggregates can only be the locus of nucleation of the polymer structure.

The lyotropic phase is retained during the reaction, but interactions between the newly formed polymer phase and the lyotropic phase result in characteristic distortions of the lyotropic phase. These distortions play an important role in the observed colloidal ordering. These distortions are analogous to interactions between a liquid crystalline phase and a second already-formed component, as described earlier for other liquid crystalline materials.[20−22] These interactions and distortions depend strongly on the nature of the liquid crystal, the surface anchoring conditions, and the particle size, and they influence dynamic processes within liquid-crystalline phases.

This interplay of colloid and liquid crystal was shown, for instance, for the alignment of colloidal droplets within a nematic phase[23] after phase separation from a homogeneous organized solution was induced by a change in temperature. In this case for a certain size of the colloidal droplets, the far field alignment of the liquid crystal can be satisfied by an alignment of the director normal to the colloid surface. This director alignment induces a hyperbolic defect. Attraction of the colloidal particles leads to the formation of linear chains or strands of colloids, and these strands are oriented parallel to the alignment direction of the liquid crystalline phase. The alignment was observed within a nematic phase between two glass slides. In this two-dimensional system a uni-dimensional orientation of the colloids occurred and linear chains formed.

There are analogies between the observations of Loudet et al.[23] and the system described here (which is three-dimensional because the polymerizations were performed in bulk phases). As a consequence, the dimensionality of the resulting morphologies increases by one and layers of linear chains are observed (Figure 6). Samples quenched during an early stage of the reaction (5 min after heating to the reaction temperature of 60 °C) show no strands but discrete polymer particles only (not shown).

Additional evidence for this proposed mechanism comes from polymerizations performed in lamellar AOT phases (UDH 62). Although the long-range order in the hexagonal phase is two-dimensional, lamellar phases are ordered in just one dimension (orthogonal to the lamellae). In this case no polymer strands were formed and only random clusters of polymer particles were observed (Figure 5d). In contrast to the polymer gels templated in hexagonal phases, there is no pronounced order on the meso scale and the polymer is isotropic and nonbirefringent. These observations are in good agree-

(20) Poulin, P. *Curr. Opin. Colloid Interface Sci.* **1999**, *4*, 66.
(21) Salamat, G.; Kaler, E. W. *Langmuir* **1999**, *15*, 5414.
(22) Zapotocky, M.; Ramos, L.; Poulin, P.; Lubensky, T. C.; Weitz, D. A. *Science* **1999**, *283*, 209.
(23) Loudet, J. C.; Barois, P.; Poulin, P. *Nature* **2000**, *407*, 611.

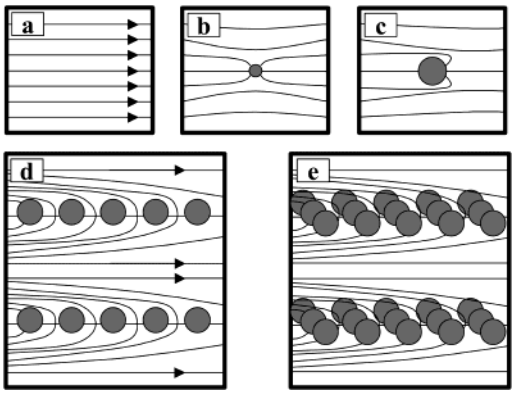

Figure 6. Proposed mechanism of the structure-directed polymerization: (a) arrows mark the director of the hexagonal phase; (b) in presence of small polymer particles just slight distortions occur; (c) for bigger particles normalization of the alignment at the particle surface takes place; (d) cooperative formation of particle chains in two dimensions; and (e) formation of layers of particle chains in three dimensions (compare also Loudet et al.[23]).

ment with investigations of colloidal particle organization in lamellar phases,[20] where only random defect network structures were found.

Kinetic Control of Morphologies. A consequence of the proposed synthesis mechanism would be a strong kinetic control of the morphologies formed because of the dynamic restructuring process within the liquid crystalline template. To investigate the influence of reaction parameters controlling the kinetics of structure formation, the concentrations of monomer and initiator, and the cross-linking degree were varied systematically.

Higher monomer contents (compared to that of UDH 12) yield more dense structures of polystyrene-*co*-divinylbenzene (Figure 5c). Lower cross-linking degrees resulted in larger and less-ordered structures, as the gel point is reached at higher conversions. For cross-linker concentrations of half that of the original sample, chain formation is less pronounced and the sheetlike morphology is less defined (UDH 22, Figure 7a). In case of polymerization without any cross-linker (UDH 24), spherical and egg-shaped polystyrene beads with diameters of about 50−200 nm were obtained (Figure 7b).

The initiator concentration also plays an important role in the structure formation. At very low initiator concentrations (UDH 31) the chains formed (Figure 7c) are less defined than those in the original sample (UDH 12). At high initiator concentration and increased polymerization rates smaller primary particles were formed, as the higher polymerization rate results in fixation of the growing polymer matrix at an earlier stage of phase separation (UDH 34). As a consequence, the alignment of strands is less pronounced, but layerlike morphologies are still formed (Figure 7d). Thus, the polymerization rate has a strong impact on the dynamic processes that are responsible for the colloidal ordering.

The influence of the locus of initiation on the polymer morphologies was investigated by comparing the polymerization initiated by a water-soluble initiator (KPS) with initiation by an oil-soluble initiator (AIBN) for samples of otherwise identical composition (UDH 12 and UDH 35). Slightly larger clusters form from initiation by AIBN. This effect might be due to the different

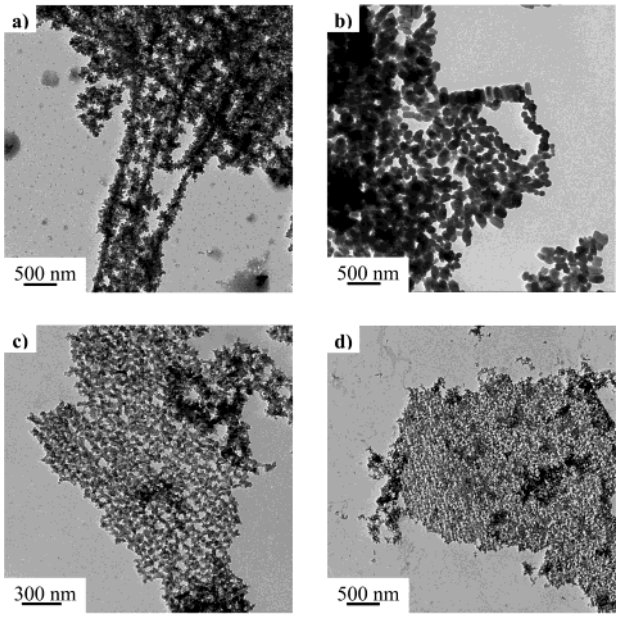

Figure 7. Polymer morphologies obtained by variation of reaction parameters: (a) larger and less-ordered structures occur at lower cross-linking degrees (UDH 22); (b) without cross-linker, spherical and egg-shaped particles are formed (UDH 24); (c) at low initiator concentrations the long-range structure is less pronounced (UDH 31); and (d) at high initiator concentrations the primary particles are too small to form well-defined particle chains (UDH 34).

dissociation rates of the initiators, or by the additional stabilization of the interface by ionic endgroups in case of initiation by KPS, but in any case the locus of initiation has no significant effect on the structure formation.

All three examples of variation of monomer, cross-linker, and initiator concentration show how the polymer morphology can be adjusted by controlling the reaction parameters that influence the kinetics of the polymerization reaction. Characterization of the polymer morphologies and the systematic variation of reaction parameters prove the dissipative character of this structure formation within lyotropic phases.

IV. Conclusion and Outlook

We have described the structure-directed synthesis of poly(divinyl benzene) and copolymers with polystyrene in inverted hexagonal phases of AOT. Colloidal ordering occurs by polymerization-induced phase separation from homogeneous self-organized solutions. By interactions with the template, the formed polymer phase induces characteristic distortions. In a nucleation and growth process morphosynthesis is directed by the anisotropic reaction field that is defined by the director of the liquid crystalline template. Polymer spheres with diameters of about 100 nm align into linear chains that form polymer layers on a micrometer scale. The hierarchical structures of the purified polymer matrix were characterized by imaging and scattering techniques (POM, SEM, TEM, and SAXS). The structure formation can be kinetically controlled by adjusting reaction parameters, such as cross-linking density, and monomer and initiator concentration.

The process is broadly similar to the colloidal ordering observed following thermally induced phase separation of silicone oils from thermotropic liquid crystals.[23] Both systems are examples of structure formation in non-equilibrium systems, a principle which is characteristic of many biological systems (morphogenesis), where structure formation takes place on various length scales and hierarchical morphologies are formed. Phase separation in structure-directing reaction fields can be used as a means for controlled structuring of matter by applying the principals of self-(re)organization.

Acknowledgment. We thank Markus Antonietti, Heimo Schnablegger, Rona Pitschke, and Bernd Smarsly for discussions and technical support. H.P.H. gratefully acknowledges financial support by the DAAD.

CM020832R